J Solid State Electrochem (2011) 15:821–827
DOI 10.1007/s10008-010-1161-2

ORIGINAL PAPER

An amperometric sensor for hydrazine based on nano-copper oxide modified electrode

Zhaojing Yin · Liping Liu · Zhousheng Yang

Received: 11 April 2010 / Revised: 7 June 2010 / Accepted: 25 July 2010 / Published online: 10 August 2010

Abstract A sensitive hydrazine sensor has been fabricated using copper oxide nanoparticles modified glassy carbon electrode (GCE) to form nano-copper oxide/GCE. The nano-copper oxide was electrodeposited on the surface of GCE in $CuCl_2$ solution at −0.4 V and was characterized by Scanning electron microscopy and X-ray diffraction. The prepared modified electrode showed a good electrocatalytic activity toward oxidation of hydrazine. The electrochemical behavior of hydrazine on nano-copper oxide/GCE was explored. The oxidative current increased linearly with improving concentration of hydrazine on nano-copper oxide/GCE from 0.1 to 600 μM and detection limit for hydrazine was evaluated to be 0.03 μM at a signal-to-noise ratio of 3. The oxidation mechanism of hydrazine on the nano-copper oxide/GCE was also discussed. The fabricated sensor could be used to determine hydrazine in real water.

Keywords Amperometric sensor · Nano-copper oxide · Hydrazine · Electrodeposition

Introduction

Hydrazine (N_2H_4) and its derivatives have been found to have wide applications in industry, agriculture, and military. Hydrazine is used in agriculture as insecticide, plant-growth regulators, propellants and pharmaceuticals [1] and its salts and methyl and dimethyl derivatives are used as rocket fuel, gas generators, and explosives. Despite the wide use of hydrazine in various areas, it has been known to be harmful to human life. Hydrazine has adverse health effect such as DNA damage [2], creation of blood abnormalities, and irreversible deterioration of nervous system [3] and it has been recognized as a carcinogenic and hepatotoxic substance which causes liver and kidney damages [4]. Thus, reliable and sensitive analytical methods for the determination of hydrazine are extremely important both in the studies of biological processes and for industrial purposes.

Classical methods and techniques are used for the detection of hydrazine such as ion chromatography [5], optical chemical sensors [6], flow injection analysis [7, 8], chemiluminescence [9], and various types of spectroscopy [10, 11]. Nevertheless, the processes involved in many of these methods are extremely complex. Among several techniques, electrochemical techniques offer the opportunity for portable, economical, sensitive, and rapid methodologies for the determination of hydrazine [12]. Chemically modified electrodes containing specifically selected redox mediators immobilized on conventional electrode materials have received increasing attentions. Recently, heat-treated cobalt tetraphenylporphyrin modified electrode [7], vitamin B12 adsorbed glassy carbon electrode [13], platinum particles-modified carbon fiber micro-electrodes [14] and NiHCF-modified graphite electrode [3] have been used to fabricate hydrazine sensors. Electro-oxidation of hydrazine at gold [15], nickel [16], and mercury [15] electrodes has also been studied. The nano-particles have been used to enhance the electron-transfer rate and to reduce the overpotential for the oxidation of hydrazine, due to the exotic properties of nanostructures [17, 18].

Metallic nanoparticles have found utility in catalytic applications. Since the surface area of a catalyst is a critical factor, metallic nanoparticles, having an immense surface

Z. Yin · L. Liu · Z. Yang (✉)
College of Chemistry and Materials Science,
Anhui Key Laboratory of chemo-Biosening,
Anhui Normal University,
Wuhu 241000, People's Republic of China
e-mail: yzhoushe@mail.ahnu.edu.cn

area compared to conventional materials, have been intensely investigated [19]. Copper oxide nanoparticles are of particular interest due to their use in heterogeneous catalysts for the oxidation of hydrocarbons [20] and carbon monoxide [21]. Zhuang et al. [22] used CuO nanorods previously for the detection of glucose by supporting the CuO nanorods on a copper electrode substrate. Miao et al. [23] prepared an electrochemical sensor based on immobilizing nano-copper oxide particles on the nafion-coated Pt electrode which showed high electrocatalytic response to H_2O_2 reduction.

In this work, we have fabricated nano-copper oxide modified glassy carbon electrode (GCE) by directly electrodeposition nano-copper oxide onto the GCE surface to obtain a sensor for hydrazine. The fabricated sensor showed excellent catalytic activity and stability for hydrazine oxidation. The electrochemical behavior of hydrazine on nano-copper oxide/GCE was explored. The nano-copper oxide could improve heterogeneous electron transfer rate of hydrazine on the electrode. The oxidative current increased linearly with improving concentration of hydrazine on nano-copper oxide/GCE, which could be applied to determine the concentration of hydrazine in sample. The fabricated sensor exhibited high selectivity and well reproducibility.

Experimental

Reagents and instrumentation

All reagents were purchased from Shanghai Chemical Reagent Company and chemicals were analytical reagent grade. They were used as received without further purifications. Stock solution of hydrazine (0.1 M) was prepared by dissolving 0.24 mL hydrazine in 50 mL water. All solutions were prepared with doubly distilled water.

Scanning electron microscopy (SEM) was obtained on S-4800 field emission scanning electron microanalyser (Hitachi, Japan). X-ray diffraction were performed with an X-ray diffraction (XRD; Shimadzu, Japan) using a Cu $K\alpha$ source (l=0.154060 nm) at 40 kV, 30 mA in the range of $20°< 2\theta <80°$ at a scan rate of $6.0°min^{-1}$. All electrochemical experiments including cyclic voltammetry (CV), amperometric response (*i-t*) and electrochemical impedance spectroscopy (EIS) were performed with CHI660 Electrochemical Analyzer (Chenhua Instruments Co., Shanghai, China). A conventional three-electrode system was used. A GCE (Ø4.0 mm) was used as the basal electrode for fabrication. An Ag/AgCl (KCl, 3.0 M) electrode and a platinum wire electrode were used as the reference electrode and the counter electrode, respectively. All experiments were carried out at ambient temperature.

Fabrication of the nano-copper oxide-modified electrode

Prior to the modification, the GCE surface was carefully polished to a mirror-like surface with aluminum (0.05 μm diameter) slurry on polishing cloth and then sonicated successively in ethanol and doubly distilled water for 5 min, respectively. Copper film was electrodeposited on the surface of the GCE by maintaining potential −0.40 V for 180 s in 0.1 M KCl solution containing 0.02 M $CuCl_2$ [24]. After that, the copper film/GCE was put in 0.1 mol L^{-1} NaOH solution and scanned repetitively for 20 cycles under potential range −0.5–0.3 V at 100 mVs^{-1}. Then, nano-copper oxide film was bound to GCE surface. After that, the electrode was rinsed with water and dried with N_2. During all experiments, the electrolyte was pre-purged with high purity N_2 for 10 min to remove O_2 and a continuous flow of N_2 gas was maintained over the solution.

Results and discussion

Characterization of the nano-copper oxide/GCE

Morphology and size of the nano-copper oxide/GCE were examined with SEM. Figure 1 showed the typical SEM

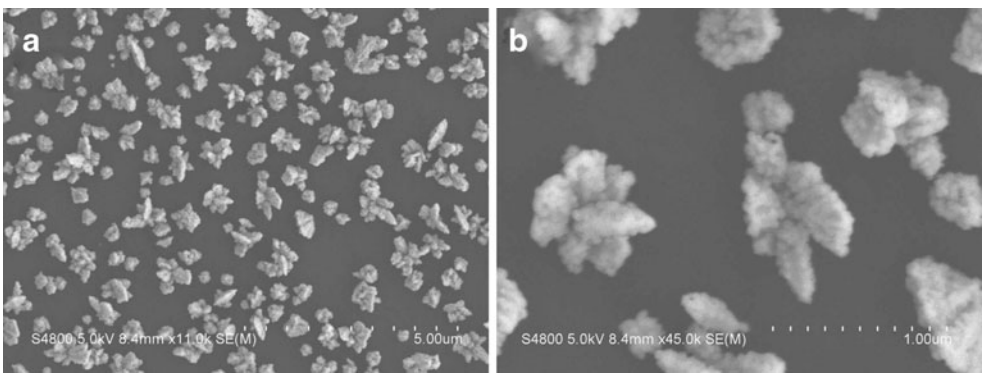

Fig. 1 SEM images of the nano-copper oxide on the surface of the GCE

images of the nano-copper oxide film on GCE. The SEM photograph illustrates that a uniform film of nano-copper oxide homogeneously distributed on the surface of GCE. The nano-copper oxide was not simple spheroid, but several small particles linked together to form a big flower-like particles. Figure 1b showed the photograph of higher magnification compare to Fig. 1a. It could be evaluated that the average size of the big particles was about 500 nm and a single small particle was about 200 nm. So the nano-copper oxide could give large specific surface area, high surface reaction activity, and efficient transmission channel for analyte molecules to reach the active sites, which will help to improve the stability and sensitivity of the modified electrode.

Figure 2 showed the XRD profiles taken from the as-prepared nano-copper oxide. All the reflections on the pattern could be indexed to the monoclinic copper oxide phase with lattice constants comparable to the reported data (JCPDS Card. No. 89–5899). By means of XRD procedure, no obvious peaks of impurity were found. This result indicates that a single phase of nano-copper oxide could be obtained by electrodeposition method.

To characterize electrochemical properties of the nano-structured copper oxide surface, CVs of an electron transfer indicator like $[Fe(CN)_6]^{3-/4-}$ was performed at the nano-copper oxide modified electrode. Figure 3a depicts the CVs of a bare GCE (curve a) and a nano-copper oxide/GCE (curve b) obtained in a 5.0 mmol/L $[Fe(CN)_6]^{3-/4-}$ solution containing 0.1 M KCl at 100 mVs^{-1}. It can be seen that the peak current (I_p) of $[Fe(CN)_6]^{3-/4-}$ increased and the peak-to-peak separation (ΔE_p) decreased in the order of bare electrode (a) and nano-copper oxide/GCE (b). A couple of well-defined peaks were observed for the nano-copper oxide/GCE with a ΔE_p of ~65 mV and a near unity of anodic-to-cathodic peak current ration $\left(I_p^a/I_p^c\right)$, indicating that the electrochemical process was quasi-reversible. EIS was also carried out to probe the interfacial electron-transfer resistance (*Ret*) at the modified electrode, whose semicircle portion corresponded to the electron transfer limited process [25]. Figure 3b shows the Nyquist diagrams of bare GCE (a) and nano-copper oxide/GCE (b) in 5.0 mmol/L $[Fe(CN)_6]^{3-/4-}$ containing 0.1 M KCl, respectively. The nano-copper oxide/GCE showed a lower interfacial electron transfer resistance (220±5Ω) than that of bare GCE (400 ± 5Ω). These facts suggest that the electron transfer is faster at the nano-copper oxide/GCE than that at bare GCE, which facilitates the arrival of the electrochemical probe to the surface of the electrode. The changes of *Ret* manifested that the directly electrodepodited nano-copper oxide was in close contact with the GCE and enhanced the transfer speed of electrons.

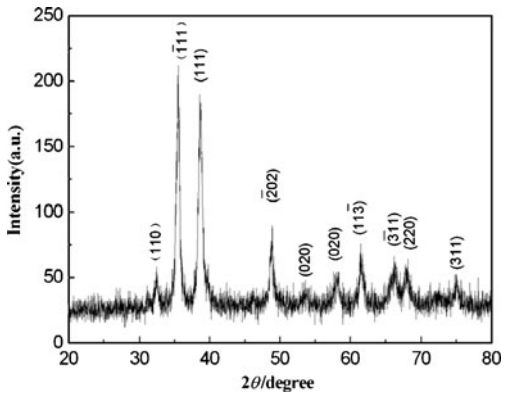

Fig. 2 XRD patterns of the nano-copper oxide

Electrochemical activity of hydrazine on nano-copper oxide/GCE

In order to investigate the electrochemical activity of N_2H_4 on the nano-copper oxide/GCE, the electrochemical response of N_2H_4 on such electrodes was explored. Figure 4 showed the typical CVs obtained at bare GCE (a) and nano-copper oxide/GCE (b) in 0.01 M NaOH solution containing

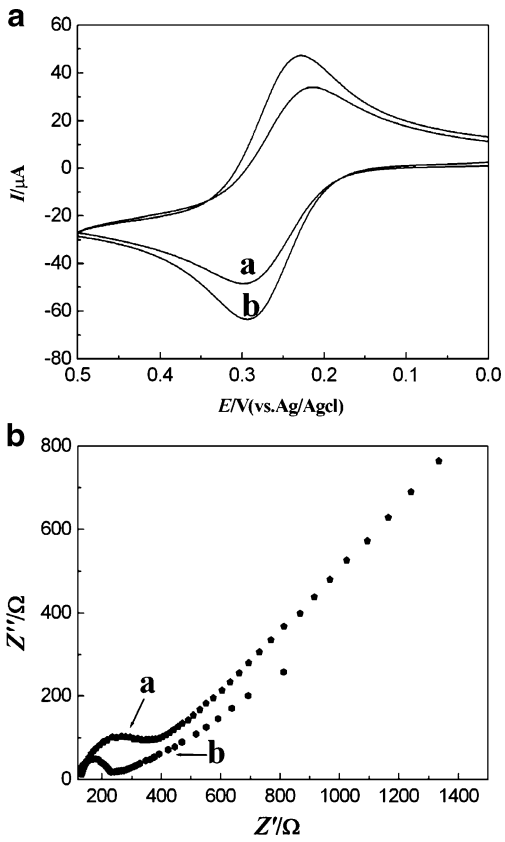

Fig. 3 **a** CVs of different modified electrodes in 5 mM$[Fe(CN)_6]^{3-/4-}$ solution containing 0.1 M KCl at a scan rate of 100 mVs^{-1} and **b** Nyquist plots at bare GCE (**a**), nano-copper oxide/GCE **b** in an aqueous solution of 5 mM$[Fe(CN)_6]^{3-/4-}$ solution containing 0.1 M KCl

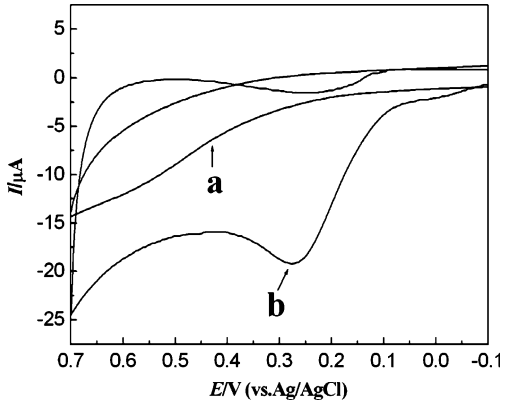

Fig. 4 Cyclic voltammograms of bare GCE **a** and nano-copper oxide/GCE **b** in 0.01 M NaOH solution containing 0.2 mM N_2H_4. Scan rate: 100 mV s^{-1}

0.2 mM N_2H_4 (at the scan rate of 100 mVs^{-1}). Only charge current was obtained at the bare GCE. However, in contrast to the bare GCE, N_2H_4 exhibited an obvious anodic peak on the nano-copper oxide/GCE. The peak potential was about 0.27 V and the peak current was about 20 μA. The oxidation of hydrazine requires very high positive overpotentials at bare GCE, as can be seen in Fig. 4 curve a, leading to a poorly defined anodic wave characteristic of very slow electrode kinetics. In contrast, the catalytic oxidation at the nano-copper oxide/GCE (Fig. 4 curve b) are much sharper and occurs at about 0.27 V much less positive potentials, which reflects a faster electron-transfer reaction on the nano-copper oxide/GCE owing to the high catalytic effect of the characteristic of nano-copper oxide. The electrochemical response was irreversible, as no cathodic current was observed during the reverse sweep. According to a previous report [24, 26], a possible

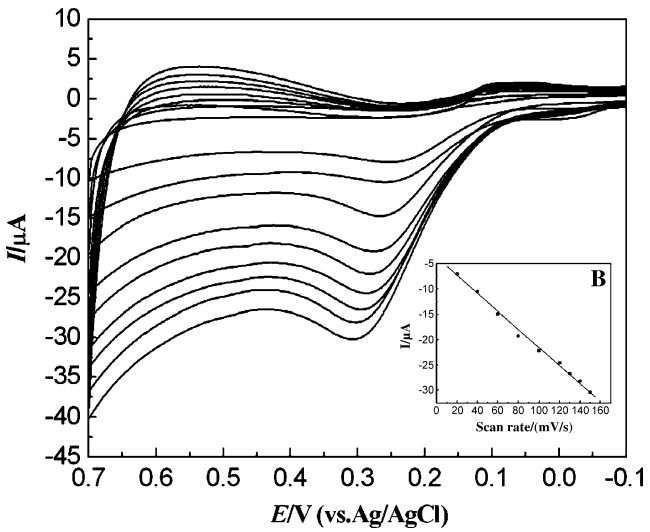

Fig. 5 CVs of nano-copper oxide modified GCE in NaOH at scan rates of 10~150 mV s^{-1} (from internal to external). *Inset b* plot of anodic peak current vs. scan rate

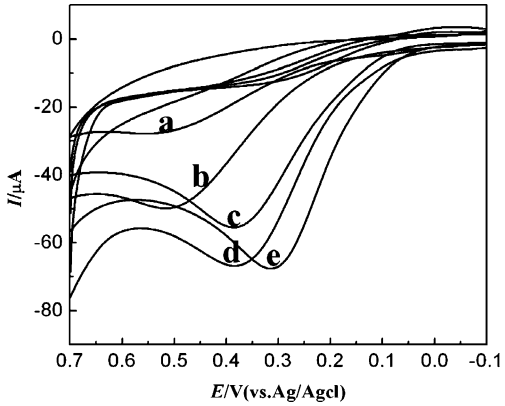

Fig. 6 Cyclic voltammograms of 0.6 mM hydrazine at the nano-copper oxide modified electrode in the presence of **a** 0.001, **b** 0.0025, **c** 0.005, **d** 0.0075, and **e** 0.01 M NaOH solution. Scan rate: 100 mV s^{-1}

electrochemical reaction for the hydrazine is proposed to be:

$$N_2H_4 + 2OH^- \rightarrow [HO - H_2NNH_2 - OH]^{2-} \quad (1)$$

$$[HO - H_2NNH_2 - OH]^{2-} + 4CuO \rightarrow 2Cu_2O + 2H_2O + 2OH^- + N_2 \quad (2)$$

$$2Cu_2O + 4OH^- \rightarrow 4CuO + 2H_2O + 4e^- \quad (3)$$

Effect of scan rate

The CVs of 0.2 mM N_2H_4 on the nano-copper oxide/GCE in 0.01 M NaOH solution at various scan rates were recorded in Fig. 5. The anodic peak currents $(I_p{}^a)$ vary linearly with the scan rate in the range of 10~150mVs^{-1}. A linear relationship between the peak current and the scan

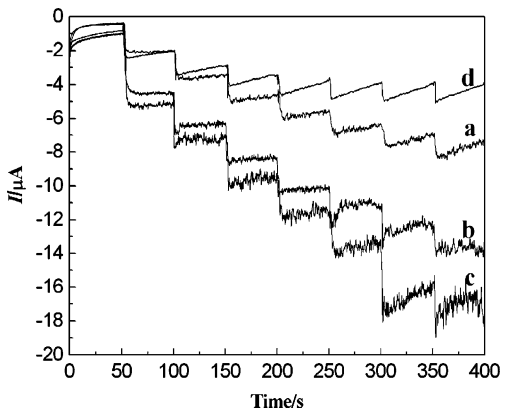

Fig. 7 Typical amperometric responses of the nano-copper oxide/GCE electrodeposited in 0.02 M $CuCl_2$ solution at 60 s (**a**), 120 s (**b**), 180 s (**c**), and 240 s (**d**)

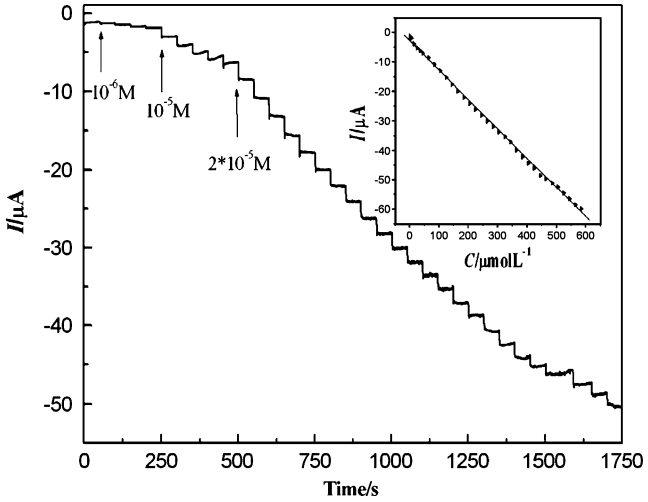

Fig. 8 Typical amperometric response of the nano-copper oxide/GCE during the successive addition of hydrazine into continuously stirred 0.01 M NaOH solution. Applied potential: +0.27 V. Inset shows plots of the peak currents as a function of concentration

rate was found as $I_p{}^a(\mu A) = -0.4031 - 0.2241V(mVs^{-1})$ ($R^2 = 0.998$). This result suggested that the electrochemical reaction process of N_2H_4 on the nano-copper oxide/GCE was a surface-controlled process. That is maybe because the Cu atom in CuO has 3D vacant orbit and the N atom in hydrazine has lone electron pair, hydrazine, and CuO attach with each other by coordinate bonds and then adsorb on the surface of electrode.

Optimization of the experimental condition

In order to obtain the optimized condition to detect hydrazine, the CVs were carried out in different concentration NaOH solution to examine the influence of NaOH solution concentration on electrochemical behavior of hydrazine on nano-copper oxide/GCE. Figure 6 showed the cyclic voltammograms of 0.6 mM hydrazine at nano-copper oxide/GCE in the presence of 0.001 (a), 0.0025 (b), 0.005 (c), 0.0075 (d), and 0.01 M (e) NaOH solution in the potential range of −100 mV to 700 mV at scan rate of 100 mVs^{-1}. The oxidative peak potential of hydrazine on nano-copper oxide/GCE shifted with changes of NaOH concentration, indicating that the formation of $[HO–H_2NNH_2–OH]^{2-}$ ion is the rate-determining step, which was coincide with the above mechanism. Further more, the peak current reached to the highest in 0.01 M NaOH solution. So we have selected 0.01 M NaOH for further investigation of the electrochemical activity of hydrazine.

The dependence of the electrochemical activity of hydrazine on the thickness of nano-copper oxide film was also examined. The electro-deposition experiments were performed at −0.4 V in the 0.02 M $CuCl_2$ solution for different times to obtain different thickness nano-copper oxide film on surface of electrode. The films obtained in these conditions completely covered the electrode surface and they are very stable from a mechanical point of view for all the considered deposition times. The effect of the film thickness on the electrochemical activity of hydrazine was evaluated with amperometric method. Figure 7 reported the amperometric response on different thickness nano-copper oxide film obtained with electro-deposition time 60 s (a), 120 s (b), 180 s (c), and 240 s (d) in 0.01 M NaOH with addition the same quantity of hydrazine each time. From 60 s to 180 s, the amperometric responses to hydrazine increased gradually and trended to stable value. By increasing the time to 240 s, the responses dramatically decreased, which could be that the nano-copper oxide film is too thick to block the electronics transmitting from hydrazine to the surface of the GCE. So, the electro-depositing time was selected to be 180 s in this work.

Amperometric determination of hydrazine

The typical amperometric response of nano-copper oxide/GCE sensor to hydrazine with the addition of successive aliquots of hydrazine in 0.01 M NaOH at an applied potential of 0.27 V was shown in Fig. 8. The response time of the fabricated sensor was less than 3 s and the inset of Fig. 8 showed the calibration graph for hydrazine determi-

Table 1 Comparison of the responses of some amperometric hydrazine sensors constructed based on different modified electrode materials

Electrode materials	E_p (V)	Detection limit (μM)	Linear range (μM)	Sensitivity (μAmM^{-1})	Ref.
Copper (hydr) oxide	0.26	–	100–1,800	–	[27]
Manganese hexacyanoferrate	0.45	6.65	33.3–8,180	47.53	[28]
Bismuth hexacyanoferrate	0.30	3	7.0–1,100	5.2	[29]
Polypyridil and phosphine Ru (II)	0.75	1	6–1,200	–	[30]
Nickel hexacyanoferrate	0.6	2.28	2–5,000	260	[31]
This work	0.27	0.03	0.1–600	94.21	–

Table 2 Effect of interfering substance on the detecting of 20 μM hydrazine. Ratio denotes the ratio of the concentration between the interfering substance and hydrazine, i.e., $[ion]/[N_2H_4]$

Species	Maximum tolerable concentration ratio
$NH_4^+Ca^{2+}$, Mg^{2+}, Al^{3+}, NO_3^-, Cl^-, Br^-, PO_4^{3-}	100
glucose, lactose, fructose	100
Pb^{2+}, Hg^+, Mn^{2+}, Cu^{2+}, Ag^+	60
Phenylhydrazine, hydroxylamine, semicarbazide	20
Fe^{2+}, Fe^{3+}, Ni^{2+}	10
$Cr_2O_7^{2-}$, NO_2^-, SO_3^{2-}	10

nation. The response of the sensor increased linearly over the hydrazine concentration range from 0.1 to 600 μM with a sensitivity of 94.21 μA mM^{-1}. The correlation coefficient of the line $R^2=0.997$ and the linear equation is $y = -3.1240 - 0.0942\times$. The detection limit is estimated to be 0.03 μM with the signal-to-noise ratio (S/N) of 3, which is lower than that of copper (hydr) oxide [27], manganese hexacyanoferrate [28], bismuth hexacyanoferrate [29], and so on (Table 1).

Anti-interference capability, reproducibility and stability of the sensor

To apply sensor for determining hydrazine in environmental water samples, the influence of some substances on determining hydrazine was examined. Various interferent-to-analyte ratios of these ions caused less than ±4% relative error for a hydrazine concentration of 20 μM. The results were listed in Table 2. It is shown that most of the examined cations and anions do not interfere with hydrazine determination. The response of the proposed sensor was essentially selective.

To characterize the reproducibility of the sensor, electrochemical experiments were repeatedly performed ten times with the same nano-copper oxide/GCE in the solution that contained 20 μM hydrazine. The experimental results showed a relative standard deviation of 2.2%, which revealed an excellent reproducibility of the present sensor. In addition, the stability of the prepared sensor was also examined by keeping the electrode in a desiccator at room temperature when not in use and recording a cyclic voltammogram each day. After sensor was used for approximately 40 times, only a small decrease of response current (about 5.8%) for 20 μM hydrazine was observed. These results indicated that the prepared sensor has a good reproducibility and stability.

Application to real water samples

In order to evaluate the validity of the proposed method for the determination of hydrazine, six water samples from three different sources were all injected with 20 μM hydrazine and were all analyzed under optimized conditions using the proposed technique. The results can be seen in Table 3. Each value is an average of five measurements and the statistical treatment of the data indicates that the results obtained by the proposed method are precise and accurate as compared with standard method.

Conclusions

A high sensitivity, fast response amperometric sensor for determining hydrazine has successfully been fabricated with electrodepositing nano-copper oxide on the surface of the GCE. The nano-copper oxide exhibited an excellent electrocatalytic activity toward hydrazine oxidation in 0.01 M NaOH solution. The hydrazine could be oxidized on nano-copper oxide at a low potential (0.27 V). The oxidative current increased linearly with improving concentration of hydrazine in the wide range with a sensitivity of 94.21 μA mM^{-1}. These features suggest that nano-copper oxide holds the promising to be a definite candidate for monitoring hydrazine in real samples.

Table 3 Results for determination of hydrazine from different water sources injected with known quantity of hydrazine

Samaple	Hydrazine Added (μM)	Hydrazine Found (μM)	Recovery (%)
Distilled water	20.00	20.36	101.8
	20.00	19.90	99.50
Drinking water	20.00	19.68	98.4
	20.00	20.32	101.6
Industrial waste water	20.00	19.92	99.6
	20.00	19.88	99.40

Acknowledgments We thank the National Natural Science Foundation of China (Grant No. 20775002) for financial support. The work was supported by Program for Innovative Research Team in Anhui Normal University.

References

1. Garrod S, Bollard ME, Nicholls AW, Connor SC, Connelly J, Nicholson J, Holmes E (2005) Chem Res Toxicol 18:115
2. Mo JW, Ogorevc B, Zhang X, Pihlar B (2000) Electroanalysis 12:48
3. Richard Prabakar SJ, Sriman Narayanan S (2008) J Electroanal Chem 617:111
4. Golabi SM, Zare HR (1999) J Electroanal Chem 465:168
5. Gilbert R, Rioux R (1984) Anal Chem 56:106
6. Ortega Barrales P, Molina Díaz A, Pascual Reguera MI, Capitan Vallvey LF (1997) Anal Chim Acta 353:115
7. Wang J, Lu Z (1989) Electroanalysis 1:517
8. Ebadi M (2003) Can J Chem 81:161
9. Huang JC, Zhang CX, Zhang ZJ (1999) Fresenius J Anal Chem 363:126
10. Safavi A, Ensafi AA (1995) Anal Chim Acta 300:307
11. Golabi SM, Zare HR (1999) Electroanalysis 11:1293
12. Ravichandran K, Baldwin RP (1983) Anal Chem 55:1782
13. Zou J, Wang E (1992) Electroanalysis 4:473
14. Zhou W, Xu L, Wu M, Wang E (1994) Anal Chim Acta 299:189
15. Korinek K, Korita J, Nusiloua M (1969) J Electroanal Chem 21:421
16. Felischmann M, Korinek K, Plrtcher D (1972) J Electroanal Chem 34:499
17. Gao GY, Guo DJ, Wang C, Li HL (2007) Electrochem Commun 9:1582
18. Christopher BM, Craig EB, Andrew OS, Timothy GJJ, Compton RG (2006) Analyst 131:106
19. Lisiecki I, Pileni MP (1993) J Am Chem Soc 115:3887
20. Reitz JB, Solomon EI (1998) J Am Chem Soc 120:11467
21. Liu Z, Zhou R, Zheng X (2007) J Mol Catal A Chem 267:137
22. Zhuang Z, Su X, Yuan H, Sun Q, Xiao D (2008) Analyst 133:126
23. Miao XM, Yuan R, Chai YQ, Shi YT, Yuan YY (2008) J Electroanal Chem 612:157–163
24. Le WZ, Liu YQ (2009) Sens Actuators B 141:147
25. Suni II (2008) TrAC Trends Anal Chem 27:604
26. Rosca V, Koper MTM (2008) Electrochim Acta 53:5199
27. Ghasem KN, Roghieh J, Parisa SD (2009) Electrochim Acta 54:5721
28. Jayasri D, Narayanan SS (2007) J Hazard Mater 144:348
29. Zheng JB, Sheng QL, Li L, Shen Y (2007) J Electroanal Chem 611:155
30. Abbaspour A, Shamsipur M, Siroueinejad A, Kia R, Raithby PR (2009) Electrochim Acta 54:2916
31. Salimi A, Abdi K (2004) Talanta 63:475